

Identification of Kynoxazine, a Novel Fluorescent Product of the Reaction between 3-Hydroxykynurenine and Erythrulose in the Human Lens, and Its Role in Protein Modification*

Received for publication, January 20, 2016, and in revised form, February 29, 2016. Published, JBC Papers in Press, March 3, 2016, DOI 10.1074/jbc.M116.716621

Stefan Rakete and Ram H. Nagaraj¹

From the Department of Ophthalmology, University of Colorado School of Medicine, Aurora, Colorado 80045

Kynurenine pathway metabolites and ascorbate degradation products are present in human lenses. In this study, we showed that erythrulose, a major ascorbate degradation product, reacts spontaneously with 3-hydroxykynurenine to form a fluorescent product. Structural characterization of the product revealed it to be 2-amino-4-(2-hydroxy-3-(2-hydroxyethyl)-2H-benzo[b][1,4]oxazin-5-yl)-4-oxobutanoic acid, which we named kynoxazine. Unlike 3-hydroxykynurenine, 3-hydroxykynurenine glucoside and kynurenine were unable to form a kynoxazine-like compound, which suggested that the aminophenol moiety in 3-hydroxykynurenine is essential for the formation of kynoxazine. This reasoning was confirmed using a model compound, 1-(2-amino-3-hydroxyphenyl)ethan-1-one, which is an aminophenol lacking the amino acid moiety of 3-hydroxykynurenine. Ultra-performance liquid chromatography-tandem mass spectrometry analyses showed that kynoxazine is present in the human lens at levels ranging from 0 to 64 pmol/mg lens. Kynoxazine as well as erythrulose degraded under physiological conditions to generate 3-deoxythreosone, which modified and cross-linked proteins through the formation of an arginine adduct, 3-deoxythreosone-derived hydroimidazolone, and a lysine-arginine cross-linking adduct, 3-deoxythreosone-derived hydroimidazolimine cross-link. Ultra-performance liquid chromatography-tandem mass spectrometry quantification showed that 32–169 pmol/mg protein of 3-deoxythreosone-derived hydroimidazolone and 1.1–11.2 pmol/mg protein of 3-deoxythreosone-derived hydroimidazolimine cross-link occurred in aging lenses. Taken together, these results demonstrate a novel biochemical mechanism by which ascorbate oxidation and the kynurenine pathway intertwine, which could promote protein modification and cross-linking in aging human lenses.

Covalent cross-linking of proteins occurs in aging lenses and strongly affects light scattering in age-related cataracts (1). Various mechanisms have been proposed for such protein cross-linking, the most prominent of which are oxidation and the Maillard reaction (2–4). In the aging lens, the levels of antiox-

idants and the activity of antioxidant enzymes progressively decline (5). These factors favor oxidative damage, although oxygen levels in the lens are relatively low (6). This finding is supported by many studies that have demonstrated the presence of oxidatively damaged proteins in human lenses (7). Furthermore, *in vitro* experiments have shown that oxidative damage to lens proteins results in their cross-linking, which underscores the important role that oxidative damage plays in the protein aggregation and light scattering that occurs in aged cataractous lenses (8).

Ascorbate is present in human lenses at high levels; concentrations of up to 3 mM have been reported (9). Ascorbate is an antioxidant and considered to protect lens constituents from oxidative damage. However, the loss of glutathione (GSH) along with a decline in the activity of glutathione reductase could promote the oxidation of ascorbate in aged and cataractous lenses (10, 11). In fact, in highly pigmented cataractous lenses, ascorbate levels are extremely low or non-existent, implying its complete or nearly complete oxidation (12). The oxidation products of ascorbate have long been known to undergo the Maillard reaction with proteins to form advanced glycation end products (AGEs)² (13). Several AGEs have been shown to occur in human lenses (3, 14). AGEs are formed as protein cross-linking and non-cross-linking adducts; many of them are fluorescent and yellow chromophores with characteristics similar to those of proteins found in aged and cataractous lenses (15).

Although it is known that ascorbate oxidation products can react with lens proteins and generate AGEs, little is known about the actual structure of such AGEs in human lenses. What has been clearly established is that to form AGEs, ascorbate must first undergo oxidation to dehydroascorbate (DHA), which, through the formation of 2,3-diketogulonate (2,3-DKG), generates a variety of highly reactive products; some of these products have been identified (16) (*e.g.* the formation of threose and erythrulose, which are strong precursors of AGEs)

* This work was supported by National Institutes of Health Grants EY022061 and EY023286 (to R. H. N.). The authors declare that they have no conflicts of interest with the contents of this article. The content is solely the responsibility of the authors and does not necessarily represent the official views of the National Institutes of Health.

¹ To whom correspondence should be addressed: Dept. of Ophthalmology, University of Colorado School of Medicine, 12800 E. 19th Ave., RC-1 North 5102, Aurora, CO 80045. Tel.: 303-724-5922; E-mail: ram.nagaraj@ucdenver.edu.

² The abbreviations used are: AGE, advanced glycation end product; 3-DT, 3-deoxythreosone; AHPE, 1-[2-hydroxy-3-(2-hydroxyethyl)-2H-1,4-benzoxazin-5-yl]ethan-1-one; DT-H, 3-deoxythreosone-derived hydroimidazolone; DOTDIC, 3-deoxythreosone-derived hydroimidazolimine cross-link; 3OHKyn, 3-hydroxykynurenine; 3OHKynG, 3-hydroxykynurenine-O-glucoside; OPD, o-phenylenediamine; MRM, multiple reaction monitoring; 2,3-DKG, 2,3-diketogulononic acid; DHA, dehydroascorbate; Q, quinoxaline; MG-H1, methylglyoxal-derived hydroimidazolone 1; MODIC, methylglyoxal-derived hydroimidazolimine cross-link; DTPA, diethylene triamine pentaacetic acid; Kyn, kynurenine; Boc, *t*-butoxycarbonyl; UPLC, ultra-performance liquid chromatography; MS², tandem MS.

(17). Furthermore, Smuda and Glomb (18) have recently identified additional AGE precursors and AGEs resulting from ascorbate oxidation. Although they studied ascorbate oxidation in the absence of proteins, the oxidation of ascorbate in the presence of proteins is likely to be different because of the reaction between the oxidation products and the proteins. The complexity of ascorbate oxidation in the presence of proteins was further illustrated by the study of Ortwerth and colleagues (19), who showed more than 100 products generated by *in vitro* incubation of ascorbate with lens proteins to be similar to products in cataractous lenses in terms of mass spectrometric characteristics.

Kynurenines are produced in the lens mainly by the kynurenine pathway initiated by indoleamine 2,3-dioxygenase (20). Kynurenines are perceived to be UV filters in the lens. However, kynurenines undergo spontaneous deamination to form α,β -unsaturated ketones that can react with nucleophilic amino acids in lens proteins and GSH (21, 22). The reaction with GSH is probably a mechanism that restricts the damaging effects of kynurenines because the latter can react with lens proteins to form adducts that can cross-link proteins (23). However, the depletion of GSH in aging and cataractous lenses could shift the balance toward the adduction of kynurenines to proteins (12). This notion is supported by findings indicating that the levels of kynurenine-adducted proteins increase with lens age and severity of cataract formation (22, 24, 25).

The kynurenine pathway and ascorbate-mediated AGE synthesis in the lens appear to be interlinked because kynurenines modulate AGEs synthesized from ascorbate (26). In addition, kynurenines become photosensitizers upon UVA light exposure and stimulate ascorbate oxidation, thereby promoting AGE synthesis in lens proteins (27). However, in those interdependent pathways, whether ascorbate oxidation products react directly with kynurenines and whether such reactions affect lens proteins have never been investigated. Herein, we report that 3-hydroxykynurenine (3OHKyn) reacts avidly with erythrose, a major ascorbate oxidation product, and forms a fluorescent adduct kynoxazine, which undergoes spontaneous degradation to form 3-deoxythresone (3-DT), which, in turn, reacts with lens proteins to form AGE adducts.

Experimental Procedures

Chemicals

3OHKyn, kynurenine (Kyn), L-erythrose, trifluoroacetic acid, methylamine hydrochloride, *o*-phenylenediamine, aminoguanidine hydrochloride, 7-azatryptophan, DTPA, EDTA, leucine aminopeptidase, carboxypeptidase Y, and GSH were obtained from Sigma-Aldrich. Methanol, acetonitrile, ethyl acetate, hexane, acetone, methylene chloride, formic acid, DMSO, 1-(2-amino-3-hydroxyphenyl)ethanone (AHPE), N^{ϵ} -carboxymethyllysine, silica gel, N^{α} -Boc-arginine, N^{α} -Boc-lysine, sodium phosphate, sodium biphosphate, sodium sulfate, Pronase E, deuterated solvents, sodium azide, and PBS were obtained from Fisher. 3-Hydroxykynurenine glucoside (3OHKynG) was synthesized as described previously (28). The quinoxalines of DHA and 2,3-DKG were prepared as described previously (16, 29).

Isolation and Characterization of 2-Amino-4-[2-hydroxy-3-(2-hydroxyethyl)-2H-1,4-benzoxazin-5-yl]-4-oxobutanoic Acid (Kynoxazine, 1) from the Reaction between Erythrose and 3-Hydroxykynurenine

Thirty-five milligrams of 3OHKyn (0.16 mmol) dissolved in 420 μ l of 0.5 M HCl was added to 500 mg (3.5 mmol) of L-erythrose in 2.1 ml of 0.1 M phosphate buffer (pH 6.0). After adjusting the pH to 6.0 with 6 M NaOH, the solution was kept at 37 °C for 30 min. Kynoxazine was purified by preparative HPLC (Method 1 (described below), retention time (t_R) = 25 min). Fractions containing kynoxazine were combined and freeze-dried to yield a yellow compound (30.6 mg, 0.1 mmol, 63%). NMR assignments are presented in Table 1. HR-MS: m/z 309.1078 (found); m/z 309.1081 (calculated for $C_{14}H_{17}N_2O_6$ [M + H]⁺).

Isolation and Characterization of 1-[2-Hydroxy-3-(2-hydroxyethyl)-2H-1,4-benzoxazin-5-yl]ethan-1-one (2) from the Reaction of Erythrose and AHPE

Ninety milligrams of AHPE (0.6 mmol) dissolved in 600 μ l of DMSO was added to 1 g (7 mmol) of L-erythrose in 4.5 ml of 0.1 M phosphate buffer (pH 5.0). The solution was kept at 37 °C for 30 min and extracted three times with 15 ml of methylene chloride. The solvent of the combined organic phases was removed under reduced pressure. The crude product was purified by column chromatography (silica gel, hexanes/acetone 2:1 (v/v), R_f = 0.39) to yield 1-[2-hydroxy-3-(2-hydroxyethyl)-2H-1,4-benzoxazin-5-yl]ethan-1-one as a yellow powder (72 mg, 0.31 mmol, 52%). NMR assignments are presented in Table 1.

Preparation of 3-DT-Quinoxaline (3-DT-Q)

Three hundred milligrams of erythrose (2.5 mmol), 170 mg of methylamine hydrochloride, and 55 mg of *o*-phenylenediamine (OPD) were dissolved in 50 ml of 0.1 M phosphate buffer (pH 7.4) and incubated for 5 days at 37 °C. The reaction mixture was extracted three times with 20 ml of ethyl acetate. The combined organic layers were dried over sodium sulfate, and the solvent was removed under reduced pressure. 3-DT-Q was obtained as a brown solid after purification by preparative HPLC (method 2, t_R = 21 min, 150 mg, 0.85 mmol, 34%). NMR spectra (¹H and ¹³C) were as described in the literature (30).

Isolation of 3-Deoxythresone-derived Hydroimidazolones (DT-Hs)

Nine hundred sixty milligrams of erythrose (8 mmol) and 930 mg (4 mmol) of N^{α} -Boc-L-arginine were dissolved in 6 ml of 0.1 M phosphate buffer containing 1 mM DTPA. The pH was adjusted to 7.4 by the addition of NaOH. The mixture was incubated for 7 days at 37 °C, fractionated by preparative HPLC (method 3, t_R = 17 min), and analyzed by UPLC-MS (m/z 359). Fractions containing the protected DT-Hs were combined and freeze-dried. After deprotection of the Boc group with 3 M HCl, individual DT-Hs were purified by preparative HPLC (method 4, t_R = 25 min). Freeze-drying of the products yielded white to yellowish solids. DT-Ha (4.5 mg, HFBA salt, 9.6 μ mol, 0.12%) and DT-Hb (9.9 mg, HFBA salt, 21.1 μ mol, 0.24%) were slightly yellow solids. DT-Hc was a slightly yellow solid (11.7 mg, HFBA

Kynoxazine in Human Lens

TABLE 1

¹H and ¹³C NMR data for kynoxazine (1) and 1-[2-hydroxy-3-(2-hydroxyethyl)-2H-1,4-benzoxazin-5-yl]ethan-1-one (2)

1		2	
¹ H	δ [ppm]	¹ H	δ [ppm]
H-1	7.50 (1H, d, $J=7.4$ Hz)	7.50 (1H, d, $J=8.4$ Hz)	
H-5	7.05 (1H, d, $J=7.6$ Hz)	6.99 (1H, d, $J=7.7$ Hz)	
H-6	6.69 (1H, d, $J=8.0$ Hz)	6.65 (1H, d, $J=7.4$ Hz)	
H-8	3.61-3.68 (2H, m)	2.55 (3H, s)	
H-9	4.29-4.35 (1H, m)	-	
H-11	4.95 (1H, pt, $J=5.0$ Hz)	4.95 (1H, d, $J=4.9$ Hz)	
H-13	2.21-2.30 (1H, m)	2.08-2.43 (2H, m)	
H-14	3.77-3.85 (2H, m)	3.75-3.85 (2H, m)	
OH (C11)	8.94 (1H, d, $J=4.9$ Hz)	9.04 (1H, d, $J=5.0$ Hz)	
¹³ C	δ [ppm]	¹³ C	δ [ppm]
C-1	123.9	C-1	125.0
C-2	116.2	C-2	117.9
C-3	141.6	C-3	141.4
C-4	134.4	C-4	133.7
C-5	121.8	C-5	121.1
C-6	116.7	C-6	115.7
C-7	197.9	C-7	200.9
C-8	39.0*	C-8	28.2
C-9	48.0	C-9	-
C-10	170.5	C-10	-
C-11	81.9	C-11	81.9
C-12	96.4	C-12	96.3
C-13	61.6	C-13	61.4
C-14	36.6	C-14	36.7

* Signal overlapped by DMSO, shift estimated from 3OHKyn NMR in D₂O.

salt, 25 μ mol, 0.31%). ¹H and ¹³C NMR data (D₂O) of DT-Hc are presented in Table 2. HR-MS (DT-Hc): m/z 259.1401 (found); m/z 259.1401 (calculated for C₁₀H₁₉N₄O₄ [M + H]⁺).

Isolation of 3-Deoxythresone-derived Hydroimidazolimine Cross-link (DOTDIC)

Seven hundred twenty milligrams of erythrose (6 mmol), 825 mg of N^α-Boc-L-arginine (3 mmol), and 738 mg (3 mmol) of N^α-Boc-L-lysine were dissolved in 6 ml of 0.1 M phosphate buffer containing 1 mM DTPA. The pH was adjusted to 7.4 by the addition of NaOH. The mixture was incubated for 7 days at 37 °C, fractionated by preparative HPLC (method 5, t_R = 27 min), and analyzed by UPLC. Fractions containing the protected DOTDIC were combined and freeze-dried. After depro-

TABLE 2

¹H and ¹³C NMR data for DT-Hc

¹ H	δ [ppm]
H-2	4.07 (1H, t, $J=6.4$ Hz)
H-3	2.01 (2H, m)
H-4	1.81 (2H, m)
H-5	3.79 (2H, m)
H-2'	4.55 (1H, t, $J=5.5$ Hz)
H-3'	2.18 (2H, m)
H-4'	3.73 (2H, m)

¹³ C	δ [ppm]
C-1	174.5
C-2	57.9
C-3	29.4
C-4	24.3
C-5	41.7
C-6	160.6
C-1'	178.5
C-2'	59.5
C-3'	34.6
C-4'	53.8

tection with 3 M HCl, DOTDIC was purified by preparative HPLC (method 4, t_R = 15 min). Freeze-drying of the product yielded a yellowish solid (4.9 mg, 0.012 mmol, 0.42%). ¹H NMR data (D₂O; Table 3) were compatible with those for a similar compound reported in the literature (31). ¹³C NMR (125 MHz, D₂O): δ (ppm) 21.9, 23.7, 27.7, 29.9, 30.1, 34.4, 42.0, 43.1, 53.8, 53.9, 60.5, 60.7, 163.5, 173.5, 180.5, 186.4. HR-MS: m/z 387.2349 (found); m/z 387.2350 (calculated for C₁₆H₃₁N₆O₅ [M + H]⁺).

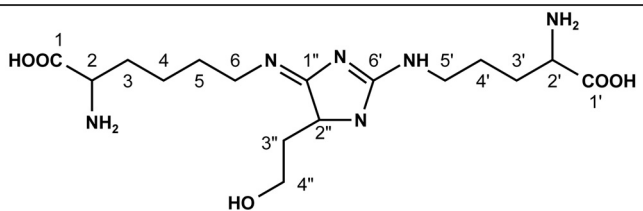
Incubation of Kynurenines and AHPE with L-Erythrose

Two millimolar 3OHKynG, 3OHKyn, Kyn, and AHPE were each incubated in 0.1 M phosphate buffer, pH 7.4, with 50 mM L-erythrose for up to 8 h. One microliter was directly used in UPLC-UV/fluorescence analyses (described below).

Stability of Kynoxazine and Identification of Degradation Products

To test its stability, kynoxazine (1 mM) was incubated under the following conditions: 1) in 0.1 M phosphate buffer, pH 7.4; 2) in argon-saturated and Chelex-treated 0.1 M phosphate buffer, pH 7.4, containing 1 mM DTPA; 3) in 0.1 M phosphate buffer, pH 7.4, containing 1 mM GSH; and 4) in 0.1 M phosphate buffer, pH 7.4, containing a water-soluble fraction of lens proteins (isolated from a 20-year-old lens at 1 mg/ml). One microliter was directly injected into a UPLC-UV/fluorescence system for analysis of kynoxazine and 3OHKyn levels (described below). 3-DT was detected as a quinoxaline derivative; to a 30- μ l sample, 3 μ l of a 55 mM OPD solution in methanol was added and incubated at room temperature for 5 h. One

TABLE 3
¹H NMR data for DOTDIC



	δ [ppm]
H-2	3.48 (1H, t, $J=7.0$ Hz)
H-3	2.00 (2H, m)
H-4	1.51 (2H, m)
H-5	1.85 (2H, m)
H-6	3.98 (2H, t, $J=6.8$ Hz)
H-2'	3.57 (1H, t, $J=6.8$ Hz)
H-3'	2.00 (2H, m)
H-4'	1.78 (2H, m)
H-5'	3.34 (2H, t, $J=6.8$ Hz)
H-2''	4.87 (1H, t, $J=5.2$ Hz)
H-3'' _A	2.00 (1H, m)
H-3'' _B	2.18 (1H, m)
H-4''	3.71 (2H, t, $J=6.2$ Hz)

microliter was directly injected into a UPLC-UV system for analysis (described below).

Incubation of α B-crystallin with Kynurenine and Erythrulose

Recombinant human α B-crystallin was purified as described previously (32). Aliquots (0.5 mg/ml) were incubated with or without 0.5 mM 3OHKynG, Kyn, 3OHKyn, erythrulose, kynoxazine, and aminoguanidine for 5 days at 37 °C in PBS containing 0.001% sodium azide (w/v). Lysine-acetylated α B-crystallin was prepared as described previously (32). For SDS-PAGE (12% gel), 7.5 μ g of protein was used. Fluorescent proteins in the gels were visualized immediately after electrophoresis in a Bio-Rad imager (excitation wavelength, 302 nm; emission wavelength, 560 nm). Thereafter, all proteins were stained with Coomassie Blue.

Isolation of Protein-free Extracts and Proteins of Human Lenses

Normal human lenses obtained from the Saving Sight (Kansas City, MO) were individually cut into two halves, and each was weighed. Kynurenines were extracted from one half as described previously (33) with some modifications. One-half of each lens was homogenized in a hand-held glass homogenizer with 500 μ l of ethanol containing 1 μ M 7-azatryptophan (internal standard). The suspension was stored at -20 °C for 30 min and centrifuged for 15 min (13,200 \times g, 4 °C). The supernatant was collected, and the pellet was suspended in 300 μ l of 80% ethanol (v/v) and processed as described above. The two supernatant fractions were pooled, and the ethanol was evaporated with a gentle stream of argon. After lyophilization of the residue, the sample was suspended in 200 μ l of 0.1% formic acid (v/v) and filtered by centrifugation using a 0.45- μ m nylon filter (Fisher). An aliquot of the filtrate was diluted with an equal

volume of acetonitrile prior to ultra-performance liquid chromatography-tandem MS (UPLC-MS²) analysis (method 1). The other half of the lens was homogenized in a hand-held glass homogenizer with 500 μ l of PBS containing 1 mM EDTA. Three hundred microliters of the homogenate was dialyzed against PBS and freeze-dried for AGE assays, and the remaining homogenate was used for dicarbonyl assays as described below.

UPLC-MS² Analysis for α -Dicarbonyls in Lens Homogenates

Dicarbonyls were trapped following a protocol described in the literature with some modifications (29). To 50 μ l of a lens homogenate prepared as described above, 30 μ l of 2 M ammonium formate buffer, pH 3, and 20 μ l of a 2.75 mM OPD solution in 0.1% HCl (v/v) were added. The samples were incubated for 24 h at room temperature in the dark. Then 25 μ l of 2 M trifluoroacetic acid was added, and samples were incubated for 1 h at room temperature. Next, 50 μ l of 3.3 M aqueous ammonia was added, and the sample was centrifuged for 15 min at 16,000 \times g. The resulting supernatant was directly used for UPLC-MS² analysis (method 2).

Incubation of Erythrulose and Kynurenines with N^{α} -Boc-protected Amino Acids

One millimolar erythrulose and kynoxazine were incubated independently with 10 mM N^{α} -Boc-arginine and N^{α} -Boc-lysine in 0.1 M phosphate buffer, pH 7.4, for 5 days at 37 °C. Fifty microliters of this reaction was deprotected with an equal volume of 6 M HCl for 30 min. The solution was neutralized, lyophilized, and dissolved in 100 μ l of 50% acetonitrile (v/v). One microliter was injected into a UPLC-MS² system (method 3).

Enzymatic Digestion of Proteins for AGE Analysis

Enzymatic digestion of lens proteins was performed as described previously with some minor modifications (14). Five hundred micrograms of freeze-dried protein was dissolved in 150 μ l of PBS, and one small crystal of thymol was added. To this solution, 0.1 units of Pronase E (two additions), 0.3 units of leucine aminopeptidase, and 0.3 units of carboxypeptidase Y were added stepwise at 24-h intervals for 96 h. Finally, the sample was filtered through a 3 kDa cut-off filter (VWR, Radnor, PA). To determine protein digestion efficiency, we compared the N^{ϵ} -carboxymethyllysine levels in the enzyme digests with those in acid hydrolysates of the same sample and considered N^{ϵ} -carboxymethyllysine levels in acid-hydrolyzed samples to represent 100% efficiency of hydrolysis, as described previously (14). A sample aliquot was diluted with an equal volume of acetonitrile prior to UPLC-MS² analysis (method 3).

Preparative High Performance Liquid Chromatography

All preparative runs were carried out with a binary pump (Waters 1525) operating at a flow rate of 15 ml/min. Samples were applied via a 2-ml injection loop (Rheodyne). Separations were carried out at room temperature on an RP C18 column (XBridge Prep C18, 250 \times 19 mm, 5 μ m; Waters) connected to a guard column. After the column, 0.3 ml/min was diverted through a valve to a UV-visible detector (Waters 2489), and the rest of the flow (14.7 ml/min) was collected in fractions. The

Kynoxazine in Human Lens

following additional conditions were used for preparative purification of individual compounds.

Method 1 (Kynoxazine)—Water (solvent A) and 80% acetonitrile (solvent B (v/v)) were used as eluents. To both solvents, 0.1% trifluoroacetic acid (v/v) was added. Analyses were performed using gradient elution: 3% B (0–10 min) to 5% B (20 min) to 15% B (30 min) to 35% B (40 min) to 65% B (50 min) to 100% B (52 to 72 min). The column was equilibrated with 3% B for 15 min prior to the next run. The detection wavelength was set to 240 nm.

Method 2 (3-DT)—Water (solvent A) and 80% acetonitrile (solvent B, (v/v)) were used as eluents. To both solvents, 0.1% formic acid (v/v) was added. Analyses were performed using gradient elution: 5% B (0–5 min) to 20% B (20 min) to 30% B (25 min) to 100% B (35–50 min). The column was equilibrated with 5% B for 15 min prior to the next run. The detection wavelength was set to 320 nm.

Method 3 (Boc-DT-H)—Water (solvent A) and 80% acetonitrile (solvent B (v/v)) were used as eluents. To both solvents, 0.1% formic acid (v/v) was added. Analyses were performed using gradient elution: 5% B (0–5 min) to 20% B (15 min) to 30% B (25 min) to 70% B (35 min) to 100% B (40–55 min). The column was equilibrated with 5% B for 15 min prior to the next run. The detection wavelength was set to 240 nm.

Method 4 (DT-H and DOTDIC)—Water (solvent A) and 80% acetonitrile (solvent B, (v/v)) were used as eluents. To both solvents, 0.1% heptafluorobutyric acid (DT-H (v/v)) or 0.1% trifluoroacetic acid (DOTDIC (v/v)) were added. Analyses were performed using gradient elution: 0.5% B (0–5 min) to 10% B (20 min) to 40% B (30 min) to 30% B (40 min) to 100% B (45 to 60 min). The column was equilibrated with 0.5% B for 15 min prior to the next run. The detection wavelength was set to 240 nm.

Method 5 (Boc²-DOTDIC)—Water (solvent A) and 80% acetonitrile (solvent B (v/v)) were used as eluents. To both solvents, 0.1% formic acid was added (v/v). Analyses were performed using gradient elution: 10% B (0–5 min) to 25% B (15 min) to 50% B (30 min) to 80% B (40 min) to 100% B (45–60 min). The column was equilibrated with 10% B for 15 min prior to the next run. The detection wavelength was set to 240 nm.

Ultra-performance Liquid Chromatography UV/Fluorescence Detection

Analysis was carried out in a Waters Acquity UPLC system (Milford, MA) connected to a UV and fluorescence detector. Chromatographic separations were carried out on an RP C-18 column (ACQUITY peptide C18 BEH, 50 × 2.1 mm, 1.7 μm; Waters) connected to a guard column at a flow rate of 0.5 ml/min. Water (solvent A) and 80% acetonitrile (solvent B (v/v)) were used as eluents. To both solvents, 0.1% trifluoroacetic acid (v/v) was added. Analyses were performed at a column temperature of 40 °C using gradient elution: 1% B (0–0.02 min) to 10% B (0.03 min) to 15% B (0.5 min) to 50% B (0.9 min) to 100% B (1.25–2.3 min). The column was equilibrated at 1% B for 1 min prior to the next analysis. Detection was achieved by setting the absorption wavelength to 360 nm for UV. For fluorescence, excitation was set to 360 nm, and emission was set to 480 nm.

Ultra-performance Liquid Chromatography UV

Analysis was carried out in a Waters Acquity UPLC system (Milford, MA) connected to a UV detector. Chromatographic separations were carried out on an RP C-18 column (ACQUITY peptide C18 BEH, 50 × 2.1 mm, 1.7 μm; Waters) connected to a guard column at a flow rate of 0.5 ml/min. Water (solvent A) and 80% acetonitrile (solvent B (v/v)) were used as eluents. To both solvents, 0.1% formic acid (v/v) was added. Analyses were performed at a column temperature of 40 °C using gradient elution: 1% B (0–0.02 min) to 10% B (0.03–0.1 min) to 15% B (0.75 min) to 40% B (1.5 min) to 70% B (2 min) to 100% B (2.3–3.5 min). The column was equilibrated at 1% B for 1 min prior to the next analysis. Detection was achieved by setting the absorption wavelength to 320 nm.

UPLC-MS²

All chromatographic analyses were carried out in a Waters Acquity UPLC system connected to a Sciex 4500 QTrap (Redwood City, CA). Mass spectrometric analyses were carried out in the multiple reaction monitoring (MRM) mode.

Method 1 (Kynurenines)—Chromatographic separations were carried out on an ACQUITY BEH Amide column (100 × 2.1 mm, 1.8 μm; Waters) connected to a guard column using a flow rate of 0.5 ml/min. Water (solvent A) and acetonitrile (solvent B) were used as eluents. To both solvents, 0.1% formic acid (v/v) was added. Analyses were performed at a column temperature of 40 °C using gradient elution: 0–10% B (0–0.25 min) to 20% B (0.75 min) to 50% B (1.6 min) to 70% B (1.8–3.5 min). The column was equilibrated at 0% B for 1 min prior to the next analysis. Detection of the analytes was achieved by using multiple reaction monitoring. The ion source was run under the following conditions: temperature, 550 °C; ion spray voltage, 4.5 kV; curtain gas, 45 ml/min; nebulizer gas, 60 ml/min; heating gas, 60 ml/min. The MRM parameters are presented in Table 4. Quantitation was performed based on the standard addition method.

Method 2 (α-Dicarbonyls)—Chromatographic separations were carried out in an ACQUITY BEH C18 peptide column (50 × 2.1 mm, 1.7 μm; Waters) connected to a guard column using a flow rate of 0.5 ml/min. Water (solvent A) and 80% acetonitrile (solvent B (v/v)) were used as eluents. To both solvents, 0.1% formic acid (v/v) was added. Analyses were performed at a column temperature of 40 °C using gradient elution: 1% B to 100% B (4 min). The column was equilibrated at 1% B for 1 min prior to the next analysis. Detection of the analytes was achieved by using multiple reaction monitoring. The ion source was run under the following conditions: temperature, 450 °C; ion spray voltage, 3.5 kV; curtain gas, 35 ml/min; nebulizer gas, 70 ml/min; heating gas, 40 ml/min. The MRM parameters are given in Table 4. Quantitation was performed based on the standard addition method.

Method 3 (AGEs)—Chromatographic separations were carried out on an ACQUITY BEH Amide column (100 × 2.1 mm, 1.8 μm; Waters) connected to a guard column using a flow rate of 0.5 ml/min. Water (solvent A) and acetonitrile (solvent B) were used as eluents. To both solvents, 0.1% formic acid (v/v) was added. Analyses were performed at a column temperature

TABLE 4

MRM parameters for kynurenine, quinoxaline, and AGE assays

DP, declustering potential; CE, collision energy; CXP, cell exit potential.

	t_R	m/z	DP	m/z	CE	CXP	m/z	CE	CXP	m/z	CE	CXP
	min		V		eV	V		eV	V		eV	V
Kynurenines (method 1)												
3OHKG	2.19	387.1	78	208.0	22.9	10.3	370.1	16.6	28.4	225.1	19.4	8.8
3OHKyn	1.46	225.1	30	110.0	20.0	3.9	162.0	30.2	7.9	190.1	23.1	6.2
Kyn	1.30	208.9	30	93.9	18.8	8.4	145.9	29.0	9.6	136.0	19.7	7.0
Kynoxazine	1.47	309.0	72	292.0	14.9	122.1	274.0	19.0	15.0	246.0	23.3	7.8
7-Azatriptophan	2.09	206.0	35	130.9	43.7	8.7	132.1	28.7	9.0	145.0	24.8	8.0
Quinoxalines (method 2)												
DHA-Q1	1.41	247.1	72	229.0	13.0	8.9	201.0	20.0	7.6	161.0	23.3	5.3
DHA-Q2	1.89	355.0	36	109.0	18.0	12.2	246.9	14.6	15.7	337.0	17.3	15.1
2,3-DKG-Q	1.37	265.0	27	185.1	21.1	6.5	161.1	26.3	5.6	156.9	32.1	5.2
3-DT-Q	1.76	175.1	60	157.0	21.9	10.9	129.0	34.0	11.6	145.0	22.0	10.3
AGEs (method 3)												
CML	1.59	205.1	40	84.1	25	13	130.1	17	11	56.1	50	10
DT-Ha	1.45	259.1	60	144.1	22.0	10.1	70.0	43.0	7.0	114.0	34.0	8.0
DT-Hb/DT-Hc	1.49	259.1	60	144.1	22.0	10.1	70.0	43.0	7.0	116.1	24.9	8.1
DOTDIC	2.25	387.1	100	342.1	35.8	12.8	297.0	46.3	11.6	227.1	44.7	11.8

of 40 °C using gradient elution: 0–70% B (0–0.2 min) to 50% B (0.2 min) to 25% B (3–4 min). The column was equilibrated at 70% B for 1 min prior to the next analysis. Detection of the analytes was achieved by using MRM. The ion source was run under the following conditions: temperature, 500 °C; ion spray voltage, 4 kV; curtain gas, 45 ml/min; nebulizer gas, 60 ml/min; heating gas, 60 ml/min. The MRM parameters are presented in Table 4. Quantitation was performed based on the standard addition method.

NMR Analysis

NMR spectra were recorded on a Varian Unity Inova 500 instrument (Varian, Palo Alto, CA) operating at 500 MHz for ^1H and 125 MHz for ^{13}C . Chemical shifts are reported relative to external tetramethylsilane.

Accurate Mass Determination (High Resolution MS)

The high resolution mass spectra were recorded on a Thermo Q Exactive mass spectrometer (Fisher) operating in positive ion mode over the scan range of 150–1000 m/z at 70,000 resolution. The electrospray ionization source was operated with a spray voltage of 4 kV along with a sheath gas pressure of 15 p.s.i. and an auxiliary gas flow rate of 5 (arbitrary units). Both source gases are nitrogen. The ion transfer capillary was held at 320 °C. 10 μM solutions of the compounds were prepared in 0.1% formic acid (v/v) and introduced into the source by direct infusion with a flow of 10 $\mu\text{l}/\text{min}$.

Statistics

The mean \pm S.D. of the specific number of experiments is indicated in the figure legends. The data were analyzed using StatView software (SAS Institute Inc., Cary, NC). Statistical significance was evaluated with a paired two-tailed t test, and differences were considered significant at $p < 0.05$.

Results

The incubation of 3OHKyn (Fig. 1, $t_R = 0.72$ min) and erythrose under physiological conditions generated a major fluorescent compound (Fig. 1, $t_R = 0.89$ min). Incubations at different pH values showed that the highest yield of the new

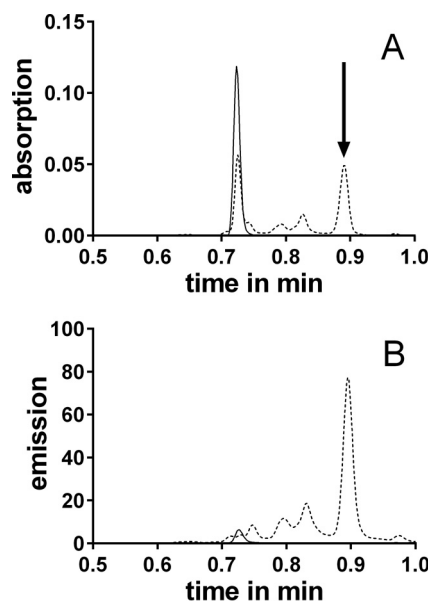


FIGURE 1. UPLC-UV (A) ($\lambda = 360$ nm) or UPLC-fluorescence (B) ($\lambda_{\text{ex}} = 360$ nm, $\lambda_{\text{em}} = 480$ nm) chromatograms of 3OHKyn-erythrose incubations at 0 (solid line) and 15 min (dashed line). The arrow indicates the peak of the major fluorescent product.

compound was observed at approximately pH 6.0 (data not shown). This product was isolated by preparative HPLC and characterized by NMR, UV, fluorescence spectroscopy, and mass spectrometry. The structure and NMR data are presented in Table 1. Homonuclear correlation spectroscopy (COSY NMR) showed four spin systems (Fig. 2). Two spin systems were assigned to the aromatic protons and the protons at the amino acid functionality of the 3OHKyn part of the molecule. A third one was assigned to the protons at the hydroxyethyl moiety. Interestingly, the last spin system was located on the heterocyclic ring. H,H-COSY experiments showed the vicinity of the protons, with shifts at 4.95 and 8.94 ppm. Heteronuclear single quantum coherence spectroscopy experiments further showed that the proton at 4.95 ppm was located on the carbon atom with a shift of 81.9 ppm. In contrast, no carbon could be assigned to the proton at 8.94 ppm. Therefore, this proton sig-

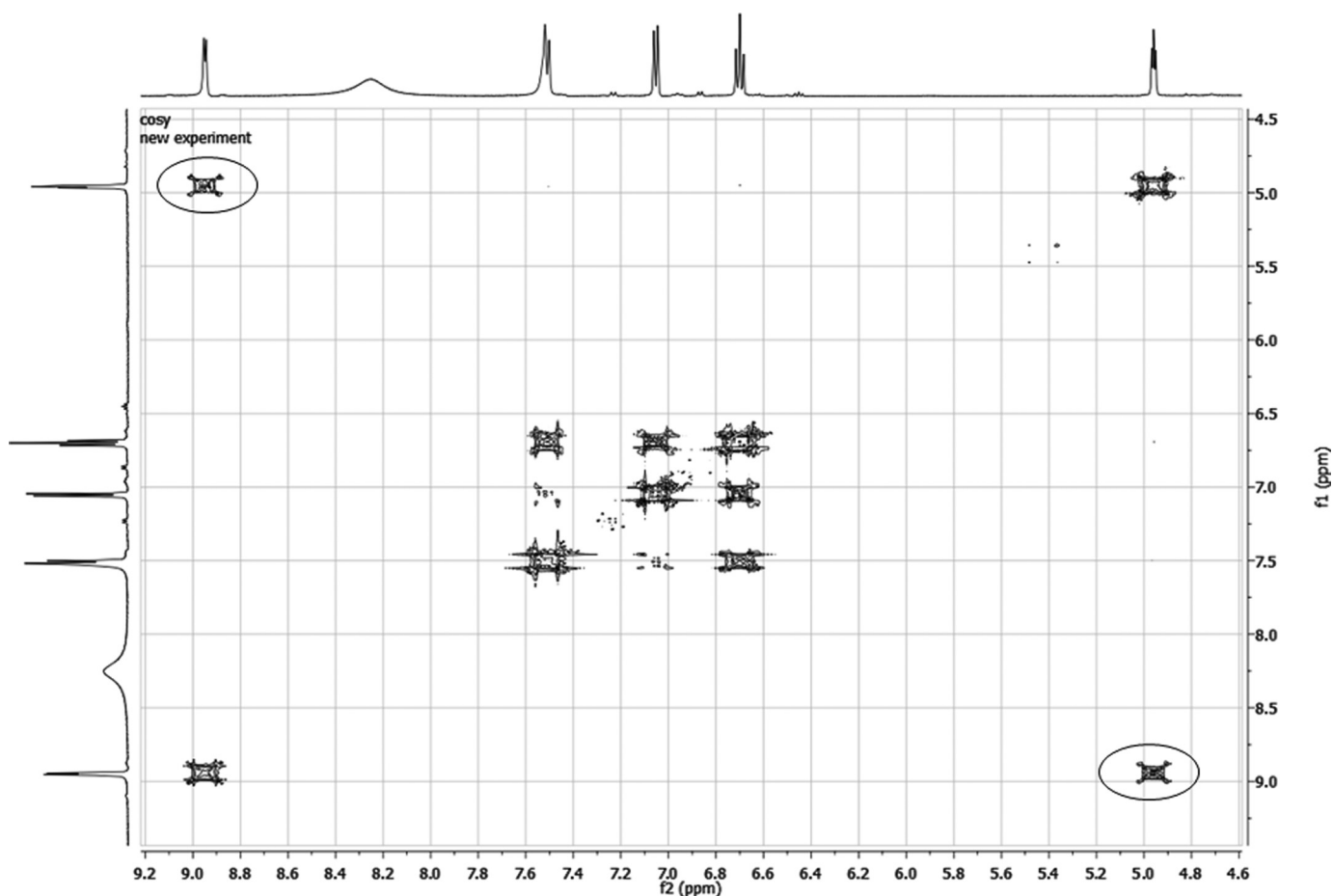


FIGURE 2. COSY NMR spectra (excerpt) of kynoxazine in D_2O . Correlations between the protons at 4.95 and 8.94 are marked with circles.

nal was assigned to the hydroxyl group at C-11. The low field shift was explained by a hydrogen bond with the ring nitrogen. The IUPAC nomenclature of this heterocyclic ring structure is 2H-1,4-benzoxazine. Based on this nomenclature and the fact that the compound was derived from 3OHKyn, we named the structure kynoxazine.

Incubation of the model compound AHPE with erythrose yielded a similar compound (structure and NMR data shown in Table 1). At pH 7.4, the absorption maximum of kynoxazine occurs at 375 nm (Fig. 3A). Kynoxazine showed fluorescence excitation and emission maxima of 375 and 495 nm, respectively (Fig. 3B).

Kynoxazine was rapidly generated in 3OHKyn-erythrose model incubations. After 15 min, the 3OHKyn level dropped to ~55% of the initial level and remained steady thereafter (Fig. 4A). At the same time, the kynoxazine level increased to ~55% of the initial 3OHKyn level and decreased to 15% thereafter. Neither 3OHKynG nor Kyn could generate kynoxazine, but their levels decreased to ~75% of the initial levels within 8 h.

The stability of kynoxazine was tested under various conditions. Interestingly, degradation of kynoxazine was not significantly affected by non-oxidative conditions, GSH, or the presence of lens proteins (Fig. 4B). The half-life of kynoxazine was determined to be ~24 h at pH 7.4 at 37 °C.

The degradation during this time yielded two major products, 3OHKyn and 3-DT (as quinoxaline derivative). UPLC-UV chro-

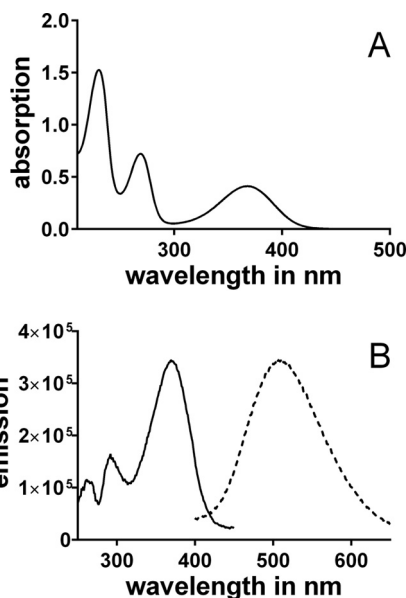


FIGURE 3. UV (A) and fluorescence (B) (solid line, excitation scan; dashed line, emission scan) spectra of 0.1 mM kynoxazine in 0.1 M phosphate buffer, pH 7.4.

matograms of kynoxazine incubations are presented in Fig. 4C. Immediately after suspension in the buffer, ~3% of kynoxazine was degraded to 3OHKyn, which increased to ~6% after 24 h of

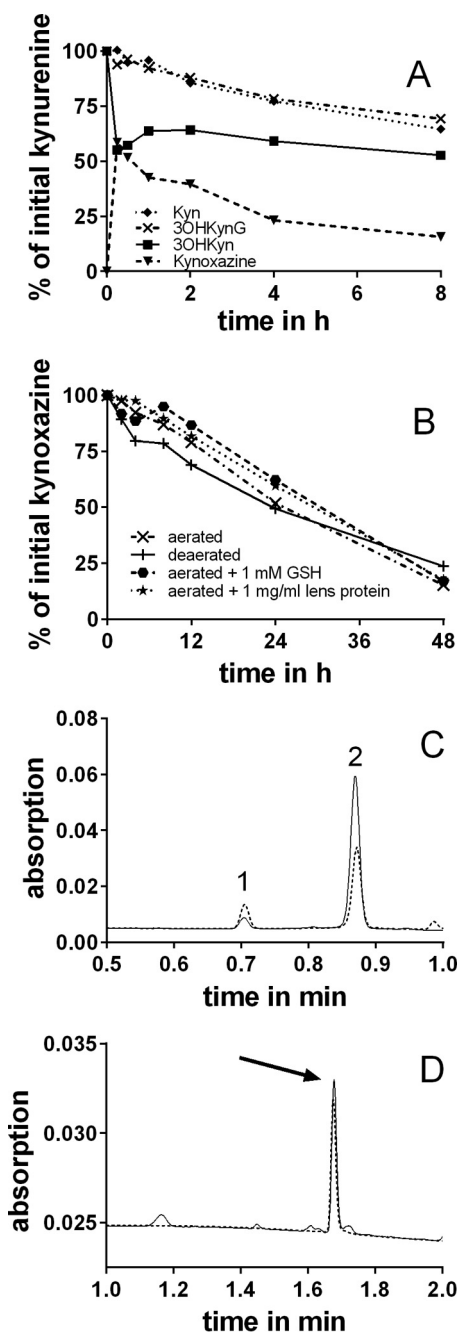


FIGURE 4. *A*, reaction of kynurenes with erythrose and formation of kynoxazine from 3OHKyn and erythrose in 0.1 M phosphate buffer, pH 7.4. Kynoxazine level is expressed as the peak area of kynoxazine relative to the initial 3OHKyn peak area. *B*, degradation of kynoxazine in 0.1 M phosphate buffer, pH 7.4, under various conditions. *C*, UPLC-UV chromatogram of kynoxazine incubations (aerated) at 0 (solid line) and 24 h (dashed line). Peak 1, 3OHKyn; peak 2, kynoxazine. *D*, UPLC-UV chromatograms of kynoxazine sample (24 h) after derivatization with OPD (solid line) and a 3-DT-Q standard (dashed line, arrow).

incubation. When a kynoxazine incubation sample was incubated further with OPD, 3-DT was the major α -dicarbonyl detected (Fig. 4*D*). Other minor degradation products were not characterized.

We detected kynoxazine in normal aging human lenses along with 3OHKynG, 3OHKyn, and Kyn. This finding was confirmed by comparing a full ion spectrum of the purified kynoxazine with a lens (from a 59-year-old donor) work-up (Fig. 5). Artificial formation of kynoxazine during lens extraction was

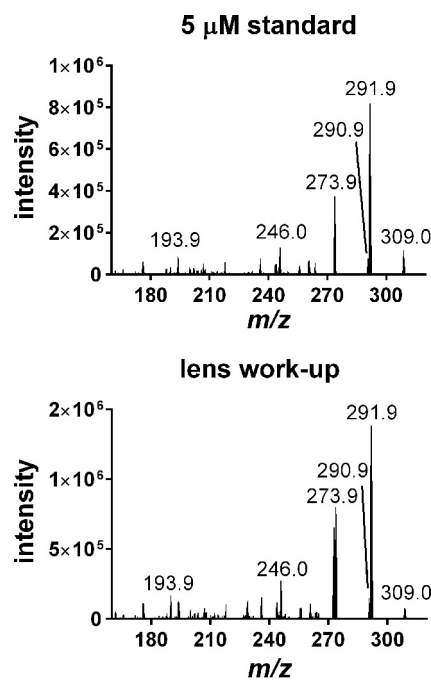


FIGURE 5. Product ion mass spectra of a kynoxazine (m/z 309.0) standard and a human lens work-up.

excluded because externally added AHPE did not lead to additional kynoxazine-like product (data not shown). However, if kynoxazine-like product (derived from AHPE/erythrose incubation) was added before lens extraction, \sim 5% of it was degraded (data not shown). This finding suggested that the levels that we detected are at least 5% lower than what would be present in an intact lens. Although kynurenes were found in all lenses, kynoxazine was present in quantifiable amounts in only 7 of 33 lenses. In six of seven lenses, the kynoxazine levels ranged from 0.44 to 0.78 pmol/mg lens wet weight, but in one lens (from the 59-year-old donor), the levels were surprisingly high at 64 pmol/mg (the 3OHKyn level in this lens was 8.4 pmol/mg lens). In other lenses, the 3OHKyn levels ranged from 1.2 to 34.2 pmol/mg lens.

The effect of kynurenes and erythrose on α B-crystallin was analyzed by SDS-PAGE. Upon incubation with 3OHKyn, erythrose, or kynoxazine, we observed cross-linked proteins with molecular mass of >25 kDa (Fig. 6*A*). Densitometric analysis showed that kynoxazine produced the highest levels of protein cross-links. Similarly, the protein fluorescence increased both in the monomeric and cross-linked proteins upon incubation with 3OHKyn or erythrose or kynoxazine. However, fluorescence was highest with kynoxazine. 3OHKynG and Kyn failed to produce similar fluorescent adducts on the protein (Fig. 6*B*). Interestingly, with 3OHKynG, a fluorescent band at \sim 25 kDa was observed, but very little protein, if any, was detected in the Coomassie-stained gel. Together, these results suggest that kynoxazine is a highly potent protein cross-linking compound that generates fluorescent adducts in such cross-linked proteins.

When aminoguanidine was added, a significant reduction in cross-linked protein was observed in incubations with erythrose or kynoxazine but not in incubations with 3OHKyn (Fig. 6*C*). However, aminoguanidine had no effect on protein fluorescence (Fig. 6*D*). When the ϵ -amino group of lysine residues in α B-crystallin were acetylated by acetic anhydride, a shift in the

Kynoxazine in Human Lens

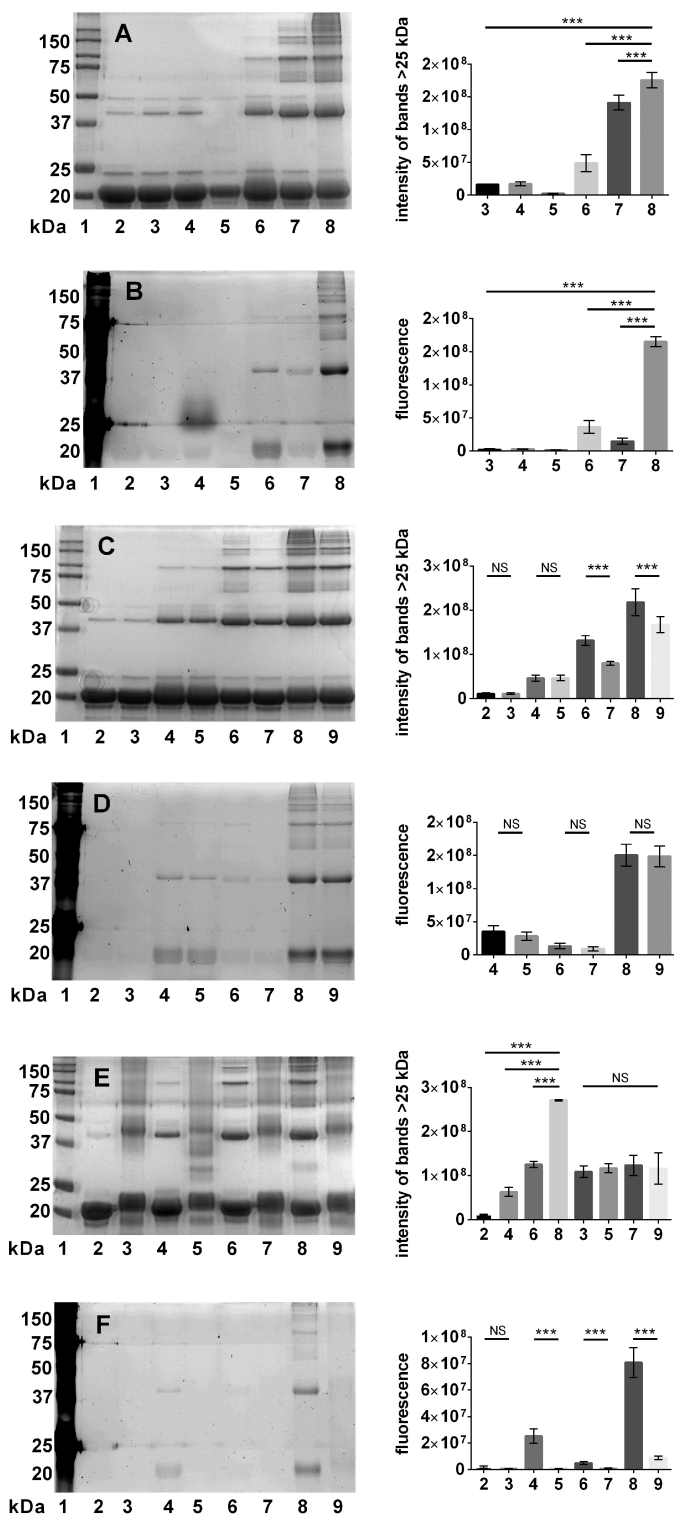


FIGURE 6. A and B, ability of kynoxazine to cross-link and form fluorescent adducts in α B-crystallin; SDS-PAGE of α B-crystallin incubated under different conditions. A, Coomassie; B, fluorescence. Lane 1, molecular weight markers; lane 2, α B-crystallin alone without incubation; lane 3, α B-crystallin alone incubated; lane 4, α B-crystallin + 3OHKynG; lane 5, α B-crystallin + Kyn; lane 6, α B-crystallin + 3OHKyn; lane 7, α B-crystallin + erythrose; lane 8, α B-crystallin + kynoxazine. C, Coomassie; D, fluorescence. Lane 1, molecular weight markers; lane 2, α B-crystallin alone incubated; lane 3, α B-crystallin + AG; lane 4, α B-crystallin + 3OHKyn; lane 5, α B-crystallin + 3OHKyn + AG; lane 6, α B-crystallin + erythrose; lane 7, α B-crystallin + erythrose + AG; lane 8, α B-crystallin + kynoxazine; lane 9, α B-crystallin + kynoxazine + AG. E, Coomassie; F, fluorescence. Lane 1, molecular weight markers; lane 2, α B-crystallin alone; lane 3, acety-

molecular mass by ~ 2 to ~ 22 kDa was observed. Furthermore, acetylated α B-crystallin showed protein bands of >25 kDa. However, when acetylated α B-crystallin was incubated with 3OHKyn, erythrose, or kynoxazine, the protein cross-linking and fluorescence were reduced when compared with those seen with the unacetylated protein (Fig. 6, E and F). Although protein cross-linking upon acetic anhydride treatment was unexpected, the lack of any further increase in protein cross-linking upon treatment with kynoxazine suggested that lysine residues are involved in kynoxazine-mediated protein cross-linking.

The ascorbate degradation products DHA, 2,3-DKG, and 3-DT were analyzed as their stable quinoxalines (Q) in lens homogenates. We did not distinguish between the free and reversibly bound ascorbate degradation products in our assay, unlike in a previous study (16). For DHA-Q, two derivatives were detected, as observed by Henning *et al.* (29). Therefore, DHA-Q levels are presented as the sum of those two derivatives. The DHA-Q levels in human lenses ranged from 9.3 to 41.5 pmol/mg lens, the 2,3-DKG-Q levels ranged from 1.3 to 28.0 pmol/mg lens, and the 3-DT-Q levels ranged from 0.06 to 0.52 pmol/mg lens. The age correlations for these degradation products are shown in Fig. 7, A–C. These results suggest that nearly 1% DHA was converted to 3-DT via 2,3-DKG in the lenses. Furthermore, 3-DT levels correlated highly with 2,3-DKG levels in the lenses (Fig. 7D).

α -Dicarbonyls, such as 3-DT, are known to form AGEs with amino acids. We isolated four AGEs from the reaction of 3-DT with N^α -Boc-lysine and N^α -Boc-arginine; three of them were arginine modifications (DT-Ha, DT-Hb, and DT-Hc), and the fourth one was a lysine-arginine cross-linking modification (DOTDIC). We were able to fully characterize only DT-Hc by NMR (Table 2), which showed chemical shifts remarkably similar to those of the previously described methylglyoxal-arginine modification, MG-H1 (34). However, results for DT-Ha and DT-Hb were inconclusive because they may represent a mixture of isomers. Nonetheless, the mass spectra of all DT-H isomers were very similar (data not shown). Only DT-Ha showed a unique fragment ion with an m/z of 114. DT-Ha and DT-Hb could not be separated by UPLC in samples, but they could be partially separated from DT-Hc. The structure of DOTDIC was confirmed by NMR (Table 3), and the results were comparable with those obtained for a compound isolated by Reihl *et al.* (31) from ascorbate incubations. The levels of total DT-H (all isomers together) were measured using the MRM transition m/z 259.1 to m/z 144.1. In the model reactions of erythrose or kynoxazine with arginine and lysine, the levels of DT-Hs were higher for erythrose at 4000 nM than for kynoxazine at 1500 nM. However, the ratio of DT-Ha and DT-Hb to DT-Hc was 1:1 in kynoxazine incubations, whereas it was 1:4 in erythrose incubations. For DOTDIC, the levels were 3 times higher

lated α B-crystallin alone; lane 4, α B-crystallin + 3OHKyn; lane 5, acetylated α B-crystallin + 3OHKyn; lane 6, α B-crystallin + erythrose; lane 7, acetylated α B-crystallin + erythrose; lane 8, α B-crystallin + kynoxazine; lane 9, acetylated α B-crystallin + kynoxazine. The bar graphs on the right show the combined densitometric values of all high molecular mass protein bands (>25 kDa), and each bar represents the mean \pm S.D. (error bars) of three independent experiments. **, $p = 0.05$; ***, $p = 0.005$; NS, not significant.

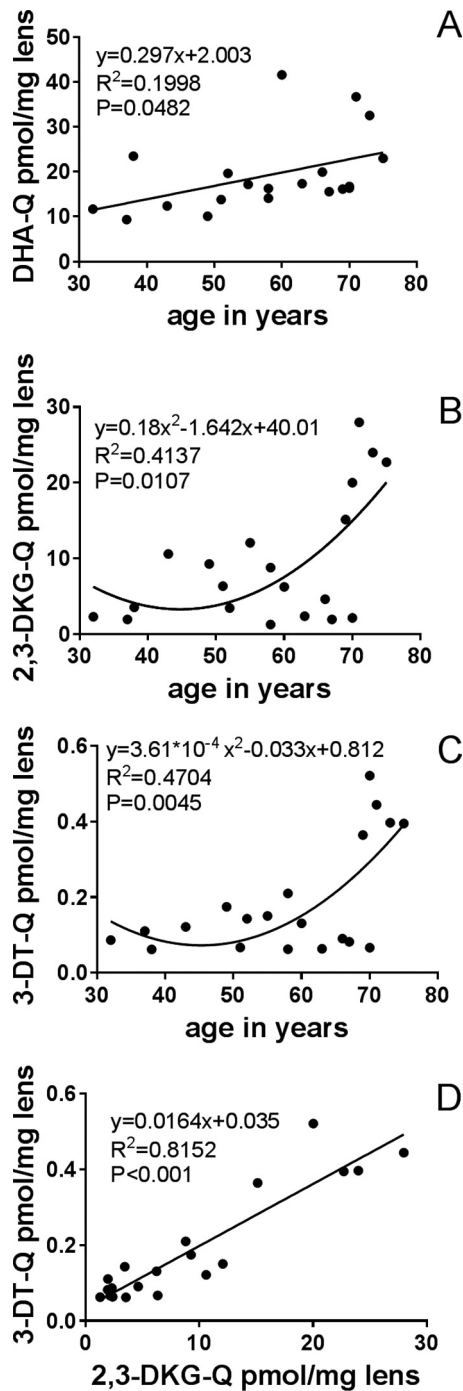


FIGURE 7. A–C, levels (pmol/mg lens) of the α -dicarbonyls (as quinoxalines) DHA (A), 2,3-DKG (B), and 3-DT (C) versus donor age for human lenses. D, correlation of 2,3-DKG-Q and 3-DT-Q with age for human lenses.

in erythrose incubations at 48 nM than in kynoxazine incubations at 16 nM.

The two AGE levels were also measured in enzymatically hydrolyzed α B-crystallin incubated with erythrose or kynoxazine. The DT-H levels in kynoxazine and erythrose incubations were 230 and 4900 pmol/mg protein, respectively. DOTDIC was only quantifiable in erythrose incubations, and the measured level was 52 pmol/mg protein.

UPLC-MS² analyses of enzyme-digested human lens proteins from 32- and 58-year-old lenses revealed the presence of

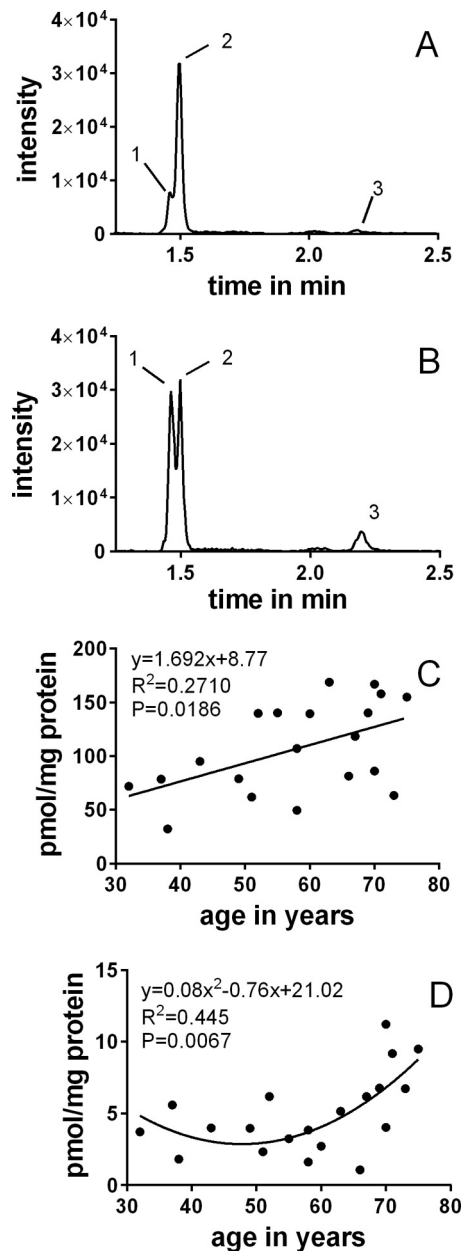


FIGURE 8. UPLC-MS² (MRM mode) chromatogram of hydrolyzed lens protein samples. A, 32 years; B, 58 years. Peak 1, DT-Ha and DT-Hb; peak 2, DT-Hc; peak 3, DOTDIC. Shown are DT-H (C) and DOTDIC (D) levels in the lens as a function of age.

the isomers of DT-H and DOTDIC (Fig. 8, A and B). The DT-H isomers were quantified in aging lenses, and the levels ranged from 32 to 169 pmol/mg protein (Fig. 8C). In some lenses, DT-Hc was the dominant isomer (e.g. in Fig. 8A), whereas in others, DT-Ha and DT-Hb were more prominent (e.g. in Fig. 8B). The levels of DOTDIC ranged from 1.1 to 11.2 pmol/mg protein (Fig. 8D). It appears that the accumulation of DOTDIC is biphasic; a steady level persists until age 50, and then an exponential increase occurs thereafter.

Discussion

The purpose of this study was to evaluate whether kynurenes and ascorbate oxidation products, both constituents of the human lens, react with each other to generate products that

Kynoxazine in Human Lens

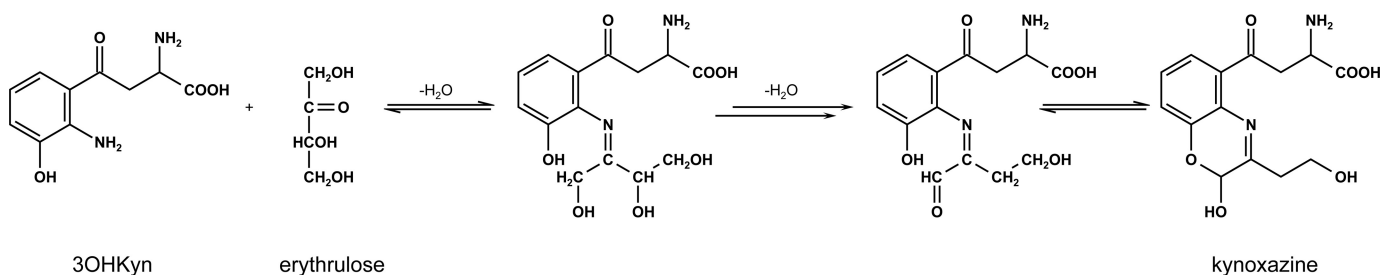


FIGURE 9. Postulated mechanism for the formation of kynoxazine from the reaction of 3OHKyn with erythrose.

negatively affect lens proteins. Our study showed that the aminophenol moiety of 3OHKyn rapidly reacts with the keto group in erythrose to form a fluorescent product. We fully characterized the product and named it kynoxazine. To confirm that the aminophenol moiety of 3OHKyn was necessary for kynoxazine formation, we incubated 3OHKynG and Kyn (both lack the aminophenol moiety but contain the α -amino group) with erythrose, and neither generated a kynoxazine-like compound. Therefore, we excluded the α -amino group on kynurenines as a participating reactant and confirmed that the aromatic hydroxyl group is necessary for the reaction. Based on the findings, we proposed a reaction mechanism for the formation of kynoxazine (Fig. 9). In this mechanism, first the aromatic amino group forms a Schiff base with erythrose. This formation is followed by a Heyns rearrangement and subsequent elimination of water in the β -position. After another rearrangement, the aldehyde group at the former C-1 of erythrose reacts with the aromatic hydroxyl group to yield kynoxazine by the intramolecular formation of a hemiacetal. Cyclic hemiacetals (lactols) are considered to be stable (35). Furthermore, NMR studies suggest an intramolecular hydrogen bond of the hydroxyl group at the C-1 of the erythrose backbone with the nitrogen located at the aromatic ring of 3OHKyn. This bond may also contribute to the stability of kynoxazine. To confirm the requirement of the aminophenol moiety, we used the model compound AHPE that contains the aminophenol moiety but lacks the α -amino group present in 3OHKyn. As expected, the structure of the condensation product of AHPE with erythrose is similar to that observed for kynoxazine. These observations explain why neither 3OHKynG nor Kyn was able to form kynoxazine with erythrose. In accord with our observation, a previous study reported the reaction of aminophenols with α -dicarbonyls (36). However, to the best of our knowledge, this is the first time a reaction of carbohydrates with an aminophenol has been reported. In contrast to the free aminophenols, oxazines derived from both 3OHKyn and AHPE show fluorescence properties that are similar to those of 3OHKynG and Kyn. It appears that the modification of the aromatic hydroxyl group by glucosylation or formation of a hemiacetal dramatically increased the fluorescence.

The formation of the hemiacetal is reversible and explains the non-quantitative reaction as well as the instability of kynoxazine. Hydrolysis of the Schiff base after ring opening yields 3OHKyn and 3-DT. Both were identified as degradation products of kynoxazine. Therefore, 3OHKyn catalyzes the dehydration of erythrose, as described for other sugars and amino acids (e.g. formation of 3-deoxyglucosone) (37). Hydroly-

sis of kynoxazine appears to be the dominant degradation mechanism because under oxidative conditions, the presence of GSH or lens proteins had no significant effect on the half-life of kynoxazine. 3OHKyn released from kynoxazine could in turn react with erythrose to generate additional kynoxazine.

The formation of 3-DT from kynoxazine was unexpected but uncovered a novel mechanism of its formation. In addition to kynoxazine, there are other potential precursors for 3-DT. In the human lens, 3-DT may be generated directly from erythrose via amine-catalyzed dehydration. However, formation from glucose is less favored (~ 0.5 mol % in glucose model incubations) (38). In contrast, model incubations of ascorbate yielded 28 mol % erythrose, which can generate 3-DT in the lens (18).

Our study established the presence of kynoxazine in human lenses, which was confirmed by mass spectrometry. However, in many lenses, kynoxazine was not present in quantifiable amounts, and there was no correlation between 3OHKyn and kynoxazine. When present, kynoxazine levels were relatively low compared with those of kynurenines (0.5 pmol/mg lens *versus* 38 pmol/mg lens Kyn) with one exception; in a 59-year-old lens, the concentration of kynoxazine was 64 pmol/mg lens. Interestingly, in the same donor's second lens, kynoxazine was not detected. Thus, kynoxazine formation varies significantly, probably as a function of the surrounding conditions, such as the concentration of erythrose and 3OHKyn and pH within the lens. However, the low levels of kynoxazine in other lenses may be explained by kynoxazine's susceptibility to hydrolysis to form 3-DT and 3OHKyn.

Kynoxazine showed a remarkably strong protein cross-linking effect, higher than that observed for kynurenines and erythrose at equimolar concentrations. When aminoguanidine, an α -dicarbonyl quencher, was added, the protein cross-linking was significantly reduced. Based on these results, it is reasonable to assume that α -dicarbonyl compounds derived from kynoxazine, possibly 3-DT, play a central role in kynoxazine-mediated protein cross-linking. Aminoguanidine did not reduce protein fluorescence, suggesting that protein-bound fluorophores are formed from precursors other than dicarbonyls. Furthermore, with acetylated α B-crystallin, in which all ϵ -NH₂ groups of lysine residues were blocked, protein cross-linking was suppressed. Therefore, lysine residues appear to be essential for the cross-linking of α B-crystallin. In addition, α B-crystallin incubated with kynoxazine became fluorescent. Interestingly, under the conditions applied, neither 3OHKynG nor Kyn showed a similar effect, despite the ability to form fluorescent adducts through the formation of α,β -unsaturated ketones that

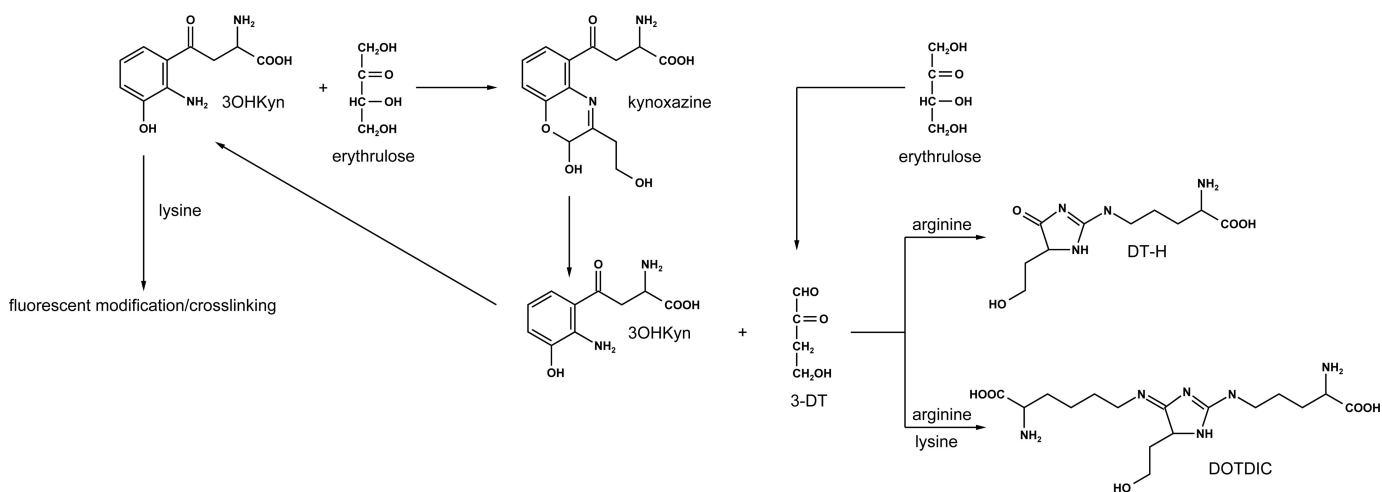


FIGURE 10. Postulated mechanism through which 3OHKyn, erythrulose, and kynoxazine modify and cross-link lens proteins.

react with nucleophilic amino acids in proteins (39). The formation of fluorescent adducts in the presence of kynoxazine is thus unlikely to be due to the reaction of deaminated kynoxazine. The formation of fluorescent adducts is probably caused by other mechanisms, which must be elucidated in future studies. Interestingly, acetylation of lysine residues inhibited the formation of fluorescent adducts in α B-crystallin incubated with kynoxazine. Therefore, lysine residues are probably involved in fluorophore formation. It is possible that 3OHKyn generated from kynoxazine could be a precursor for fluorescent products (independent of its ability to form fluorescent adducts through an α,β -unsaturated ketone, for the reasons stated above). 3OHKyn is highly redox-active and, through an intermediate, can react with lysine residues to yield fluorescent adducts. These adducts may also cross-link proteins. One possible mechanism through which 3OHKyn can cross-link peptides was reported in the study by Aquilina *et al.* (40), in which two glycine residues were cross-linked by 3OHKyn.

We demonstrated that α -dicarbonyls are involved in the cross-linking of α B-crystallin by kynoxazine. Therefore, we analyzed the total levels of α -dicarbonyls related to ascorbate degradation as their stable quinoxalines. DHA is formed by the oxidation of ascorbate. GSH reductase is able to reduce dehydroascorbate by using GSH. However, as lenses age, oxidative processes increase. In addition, the activity of GSH reductase activity as well as GSH levels decrease in the aging lens (10), and therefore, DHA levels increase (11). When reduction mechanisms begin to fail, DHA irreversibly hydrolyzes to 2,3-DKG. In the lenses we analyzed, 2,3-DKG levels showed only a weak correlation until an age of \sim 70 years. Beyond that age, 2,3-DKG levels increased dramatically, suggesting a rapid loss in the DHA reduction mechanism at advanced ages of the lens. 2,3-DKG further hydrolyzes to yield erythrulose, which dehydrates to 3-DT, possibly catalyzed by 3OHKyn or other amines. Therefore, it is reasonable to assume that 3-DT is mainly generated from 2,3-DKG. Moreover, a previous study demonstrated that 3-DT is the dominant free and protein-bound α -dicarbonyl in human lenses (16).

α -Dicarbonyls are major precursors of AGEs (14). Several α -dicarbonyls, such as methylglyoxal and glyoxal, have been

extensively studied in AGE formation (41). However, to date, specific 3-DT-derived AGEs have not been identified in proteins. Because 3-DT is a major dicarbonyl released from kynoxazine, we set out to determine the structure of AGEs derived from it. To this end, we incubated kynoxazine and erythrulose with lysine and arginine and screened for 3-DT amino acid modifications. For methylglyoxal, MG-H1 and its isomers and MODIC are the dominant and well described AGEs (42, 43). We hypothesized that 3-DT would also generate similar AGEs. In fact, we isolated three AGEs similar to MG-H1 and one MODIC-like AGE, which we named DT-H and DOTDIC, respectively. For the DT-H, we named the isomers a, b, and c, according to their UPLC elution pattern. However, only DT-Hc was unambiguously identified as the *exo*-imidazolinone that is similar to MG-H1. The other two isomers are likely to be the *endo*-imidazolinones. Arginine-modified DT-H and arginine-lysine cross-linked DOTDIC have been reported: DT-H as part of a patent and DOTDIC as a product of ascorbic acid incubations in the presence of amino acids (31, 44). However, this study represents the first time that both modifications have been identified in proteins. Because we observed that 3-DT levels increased with age, especially with advanced age, we expected 3-DT-AGEs levels to increase with age as well. In fact, DT-H and DOTDIC levels positively correlated with age. However, DT-H did not show the same enhanced accumulation during advanced age. This finding could be due to slow reaction kinetics or the binding of 3-DT to amino acids other than arginine or further degradation of 3-DT. However, the levels of DT-H and DOTDIC were lower than those measured for the MG-H1 isomers (32–169 pmol/mg lens *versus* 229–9872 pmol/mg lens (14, 42)) and MODIC (1.1–11.2 pmol/mg lens *versus* 1.3–89 pmol/mg lens (14)) in human lenses. Nonetheless, our study established that 3-DT modifications are present in human lenses at appreciable levels.

Modification of amino acid residues can drastically alter the function of proteins; in particular, arginine modification can alter hydrogen bonding with other amino acids. Previous studies have shown that point mutation of arginine in α B-crystallin causes loss of chaperone function and aggregation (45). If arginine residues are blocked by 3-DT-derived hydroimidazolino-

Kynoxazine in Human Lens

nes, the function of α B-crystallin may be compromised. Moreover, DOTDIC is a cross-linking structure formed from kynoxazine. It is possible that other cross-linking structures exist, which could include the complete kynoxazine structure or structures derived directly from 3OHKyn. Thus, kynoxazine, through the formation of 3-DT and 3OHKyn, could cause protein cross-linking and possibly protein aggregation in the lens (Fig. 10).

In conclusion, we have presented a novel mechanism by which 3OHKyn and erythrulose, an ascorbate degradation product, are chemically intertwined to induce changes in lens proteins. Our study showed that kynoxazine is a strong protein-modifying agent generated through the formation of two AGEs via 3-DT. Because erythrulose and 3-DT are primarily generated by ascorbate degradation, DT-H and DOTDIC represent novel AGE markers for ascorbate degradation in the human lens. Their formation in lens proteins could lead to aggregation and contribute to cataract formation. It is possible that kynoxazine-mediated protein modification could be augmented during cataract formation because UVA light, which is one of the causative factors for cataracts, has been shown to enhance ascorbate oxidation in the lens (27).

Author Contributions—S. R. and R. H. N. designed the work. S. R. carried out the experiments. S. R. and R. H. N. wrote the manuscript. The authors have read and approved the final manuscript.

Acknowledgments—We thank Drs. Rooban Nahomi, Johanna Rankenberg, and Cibin Raghavan for critical reading of the manuscript. We also thank Dr. Julie Haines (University of Colorado School of Medicine Metabolomics Core) for recording the high resolution mass spectra.

References

1. Chen, Y. C., Reid, G. E., Simpson, R. J., and Truscott, R. J. W. (1997) Molecular evidence for the involvement of α crystallin in the coloration/crosslinking of crystallins in age-related nuclear cataract. *Exp. Eye Res.* **65**, 835–840
2. Fu, S., Dean, R., Southan, M., and Truscott, R. (1998) The hydroxyl radical in lens nuclear cataractogenesis. *J. Biol. Chem.* **273**, 28603–28609
3. Nagaraj, R. H., Linetsky, M., and Stitt, A. W. (2012) The pathogenic role of Maillard reaction in the aging eye. *Amino Acids* **42**, 1205–1220
4. Truscott, R. J. W. (2005) Age-related nuclear cataract: oxidation is the key. *Exp. Eye Res.* **80**, 709–725
5. Tessier, F., Moreaux, V., Birlouez-Aragon, I., Junes, P., and Mondon, H. (1998) Decrease in vitamin C concentration in human lenses during cataract progression. *Int. J. Vitam. Nutr. Res.* **68**, 309–315
6. McNulty, R., Wang, H., Mathias, R. T., Ortwerth, B. J., Truscott, R. J. W., and Bassnett, S. (2004) Regulation of tissue oxygen levels in the mammalian lens. *J. Physiol.* **559**, 883–898
7. Fan, X., Zhang, J., Theves, M., Strauch, C., Nemet, I., Liu, X., Qian, J., Giblin, F. J., and Monnier, V. M. (2009) Mechanism of lysine oxidation in human lens crystallins during aging and in diabetes. *J. Biol. Chem.* **284**, 34618–34627
8. Zigler, J. S., Jr., Huang, Q. L., and Du, X. Y. (1989) Oxidative modification of lens crystallins by hydrogen peroxide and chelated iron. *Free Radic. Biol. Med.* **7**, 499–505
9. Varma, S. D., and Richards, R. D. (1988) Ascorbic acid and the eye lens. *Ophthalmic Res.* **20**, 164–173
10. Rogers, K. M., and Augusteyn, R. C. (1978) Glutathione reductase in normal and cataractous human lenses. *Exp. Eye Res.* **27**, 719–721
11. Ortwerth, B. J., and Olesen, P. R. (1988) Glutathione inhibits the glycation and crosslinking of lens proteins by ascorbic acid. *Exp. Eye Res.* **47**, 737–750
12. Tsentulovich, Y. P., Verkhovod, T. D., Yanshole, V. V., Kiryutin, A. S., Yanshole, L. V., Fursova, A. Z., Stepakov, D. A., Novoselov, V. P., and Sagdeev, R. Z. (2015) Metabolomic composition of normal aged and cataractous human lenses. *Exp. Eye Res.* **134**, 15–23
13. Ortwerth, B. J., and Olesen, P. R. (1988) Ascorbic acid-induced crosslinking of lens proteins: evidence supporting a Maillard reaction. *Biochim. Biophys. Acta* **956**, 10–22
14. Smuda, M., Henning, C., Raghavan, C. T., Johar, K., Vasavada, A. R., Nagaraj, R. H., and Glomb, M. A. (2015) Comprehensive analysis of Maillard protein modifications in human lenses: effect of age and cataract. *Biochemistry* **54**, 2500–2507
15. Cheng, R., Lin, B., Lee, K.-W., and Ortwerth, B. J. (2001) Similarity of the yellow chromophores isolated from human cataracts with those from ascorbic acid-modified calf lens proteins: evidence for ascorbic acid glycation during cataract formation. *Biochim. Biophys. Acta* **1537**, 14–26
16. Nemet, I., and Monnier, V. M. (2011) Vitamin C degradation products and pathways in the human lens. *J. Biol. Chem.* **286**, 37128–37136
17. Simpson, G. L. W., and Ortwerth, B. J. (2000) The non-oxidative degradation of ascorbic acid at physiological conditions. *Biochim. Biophys. Acta* **1501**, 12–24
18. Smuda, M., and Glomb, M. A. (2013) Maillard degradation pathways of vitamin C. *Angew. Chem. Int. Ed. Engl.* **52**, 4887–4891
19. Cheng, R., Feng, Q., and Ortwerth, B. J. (2006) LC-MS display of the total modified amino acids in cataract lens proteins and in lens proteins glycosylated by ascorbic acid *in vitro*. *Biochim. Biophys. Acta* **1762**, 533–543
20. Wood, A. M., and Truscott, R. J. W. (1993) UV filters in human lenses: tryptophan catabolism. *Exp. Eye Res.* **56**, 317–325
21. Vazquez, S., Aquilina, J. A., Jamie, J. F., Sheil, M. M., and Truscott, R. J. W. (2002) Novel protein modification by kynurenic acid in human lenses. *J. Biol. Chem.* **277**, 4867–4873
22. Korlimbinis, A., Aquilina, J. A., and Truscott, R. J. W. (2007) Protein-bound UV filters in normal human lenses: the concentration of bound UV filters equals that of free UV filters in the center of older lenses. *Invest. Ophthalmol. Vis. Sci.* **48**, 1718–1723
23. Aquilina, J. A., Carver, J. A., and Truscott, R. J. W. (2000) Polypeptide modification and cross-linking by oxidized 3-hydroxykynurenic acid. *Biochemistry* **39**, 16176–16184
24. Staniszewska, M. M., and Nagaraj, R. H. (2005) 3-Hydroxykynurenic acid-mediated modification of human lens proteins: structure determination of a major modification using a monoclonal antibody. *J. Biol. Chem.* **280**, 22154–22164
25. Staniszewska, M., and Nagaraj, R. H. (2007) Detection of kynurenic acid modifications in proteins using a monoclonal antibody. *J. Immunol. Methods* **324**, 63–73
26. Nagaraj, R. H., Padmanabha, S., Mailankot, M., Staniszewska, M., Mun, L. J., Glomb, M. A., and Linetsky, M. D. (2010) Modulation of advanced glycation endproduct synthesis by kynurenic acid in human lens proteins. *Biochim. Biophys. Acta* **1804**, 829–838
27. Linetsky, M., Raghavan, C. T., Johar, K., Fan, X., Monnier, V. M., Vasavada, A. R., and Nagaraj, R. H. (2014) UVA light-excited kynurenic acid oxidize ascorbate and modify lens proteins through the formation of advanced glycation end products: implications for human lens aging and cataract formation. *J. Biol. Chem.* **289**, 17111–17123
28. Manthey, M. K., Jamie, J. F., and Truscott, R. J. W. (1999) Synthesis of human ultraviolet filter compounds: O- β -D-glucopyranosides of 3-hydroxykynurenic acid and 2-amino-3-hydroxy- γ -oxobenzenebutanoic acid. *J. Org. Chem.* **64**, 3930–3933
29. Henning, C., Liehr, K., Girndt, M., Ulrich, C., and Glomb, M. A. (2014) Extending the spectrum of α -dicarbonyl compounds *in vivo*. *J. Biol. Chem.* **289**, 28676–28688
30. Usui, T., Yanagisawa, S., Ohguchi, M., Yoshino, M., Kawabata, R., Kishimoto, J., Arai, Y., Aida, K., Watanabe, H., and Hayase, F. (2007) Identification and determination of α -dicarbonyl compounds formed in the degradation of sugars. *Biosci. Biotechnol. Biochem.* **71**, 2465–2472
31. Reihl, O., Lederer, M. O., and Schwack, W. (2004) Characterization and detection of lysine–arginine cross-links derived from dehydroascorbic acid. *Carbohydr. Res.* **339**, 483–491

32. Nagaraj, R. H., Nahomi, R. B., Shanthakumar, S., Linetsky, M., Padmanabha, S., Pasupuleti, N., Wang, B., Santhoshkumar, P., Panda, A. K., and Biswas, A. (2012) Acetylation of α A-crystallin in the human lens: effects on structure and chaperone function. *Biochim. Biophys. Acta* **1822**, 120–129
33. Streete, I. M., Jamie, J. F., and Truscott, R. J. W. (2004) Lenticular levels of amino acids and free UV filters differ significantly between normals and cataract patients. *Invest. Ophthalmol. Vis. Sci.* **45**, 4091–4098
34. Ahmed, N., Argirov, O. K., Minhas, H. S., Cordeiro, C. A. A., and Thornalley, P. J. (2002) Assay of advanced glycation endproducts (AGEs): surveying AGEs by chromatographic assay with derivatization by 6-aminoquinolyl-*N*-hydroxysuccinimidyl-carbamate and application to N^{ϵ} -carboxymethyl-lysine- and N^{ϵ} -(1-carboxyethyl)lysine-modified albumin. *Biochem. J.* **364**, 1–14
35. Coote, S. C., Smith, L. H. S., and Procter, D. J. (2010) Product class 17: acyclic hemiacetals, lactols, and carbonyl hydrates. in *Science of Synthesis* (Ishihara, K., ed), pp. 417–473, Georg Thieme Verlag KG, Stuttgart, Germany
36. Belgodere, E., Bossio, R., Parrini, V., and Pepino, R. (1977) Condensation of *o*-aminophenol and α -dicarbonyl compounds. Part 1: benzoxazines. *J. Heterocycl. Chem.* **14**, 997–1001
37. Ledl, F., and Schleicher, E. (1990) Die Maillard-Reaktion in Lebensmitteln und im menschlichen Körper: neue Ergebnisse zu Chemie, Biochemie und Medizin. *Angew. Chem.* **102**, 597–626
38. Gobert, J., and Glomb, M. A. (2009) Degradation of glucose: reinvestigation of reactive α -dicarbonyl compounds. *J. Agric. Food Chem.* **57**, 8591–8597
39. Tsentlovich, Y. P., Sherin, P. S., Kopylova, L. V., Cherepanov, I. V., Grilj, J., and Vauthey, E. (2011) Photochemical properties of UV filter molecules of the human eye. *Invest. Ophthalmol. Vis. Sci.* **52**, 7687–7696
40. Aquilina, J. A., Carver, J. A., and Truscott, R. J. W. (1999) Elucidation of a novel polypeptide cross-link involving 3-hydroxykynurenine. *Biochemistry* **38**, 11455–11464
41. Thornalley, P. J., Battah, S., Ahmed, N., Karachalias, N., Agalou, S., Babaei-Jadidi, R., and Dawnay, A. (2003) Quantitative screening of advanced glycation endproducts in cellular and extracellular proteins by tandem mass spectrometry. *Biochem. J.* **375**, 581–592
42. Ahmed, N., Thornalley, P. J., Dawczynski, J., Franke, S., Strobel, J., Stein, G., and Haik, G. M. (2003) Methylglyoxal-derived hydroimidazolone advanced glycation end-products of human lens proteins. *Invest. Ophthalmol. Vis. Sci.* **44**, 5287–5292
43. Biemel, K. M., Friedl, D. A., and Lederer, M. O. (2002) Identification and quantification of major Maillard cross-links in human serum albumin and lens protein: evidence for glucosepane as the dominant compound. *J. Biol. Chem.* **277**, 24907–24915
44. Yamada, K., Koyama, N., Nomura, K., and Ota, M. (November 17, 2011) International Patent JP2011231022 (A)
45. Vicart, P., Caron, A., Guicheney, P., Li, Z., Prévost, M.-C., Faure, A., Chateau, D., Chapon, F., Tomé, F., Dupret, J.-M., Paulin, D., and Fardeau, M. (1998) A missense mutation in the α B-crystallin chaperone gene causes a desmin-related myopathy. *Nat. Genet.* **20**, 92–95